BULLETIN OF THE EARTHQUAKE
RESEARCH INSTITUTE
Vol. 36 (1958), pp. 71-98

5. *Spectral Study of Near Earthquake Waves (1).*

By Keiiti AKI, Masaru TSUJIURA, Minoru HORI and Kenichi GOTÔ,

Earthquake Research Institute.

(Read January 28, 1958.—Received March 31, 1958.)

1. Introduction

Many studies have been made of complicated seismograms of near earthquakes from the viewpoint of "phase", but we do not yet have any satisfactory knowledge about the nature of the waves prevailing over various portions of such seismograms. For instance, the vibrations following the initial P wave called preliminary tremors are believed by some to be the mixture of waves which started from the origin at the same time as the initial P wave and travelled along a number of different paths, while others believe that they are secondary waves, whether surface waves or local surface vibrations, generated at some places by the incidence of primary waves coming from the origin. Also, it is not impossible to presume that they are primary waves which have travelled along the same path as the initial P wave, and are due to the events which occurred after the initial breakdown at the origin of earthquake.

The question of this kind may be asked about every portion of a near earthquake seismogram, especially about the origin of its coda portion. The reason why those questions can not yet be settled seems to be owing to the lack of an appropriate method of dealing with such complicated waves.

Recently one of the present writers, K. Aki[1] (1957), proposed a useful method of revealing the nature of these complicated waves, and applied it successfully to microtremors in the city area. Since in the method the relation between the spatial spectrum and the frequency spectrum of waves plays an important part, it is necessary to assume the waves in question as stationary in space and time at least within the range to be studied. This assumption represents quite an opposite extremity when compared with that underlying the ordinary "phase" method. An earthquake wave as a whole is certainly not stationary in

1) K. AKI, *Bull. Earthq. Res. Inst.*, **35** (1957), 415-456.

time, but it may be possible to divide the wave into consecutive portions, within each of which the wave can be safely assumed as stationary.

The present paper is a preliminary report in which an application of the spectral method is attempted for seismic waves of near earthquakes in order to give an answer to the above question.

A tripartite system of seismometers were set up at Kamakura, in Kanagawa Prefecture. The vibrations of three seismometers caused by earthquakes are recorded simultaneously, by the use of a frequency modulation, on a magnetic tape. The analyses according to the method are applied to the vibrations, reproduced afterwards in our laboratory, with the aid of filters and a correlation computer.

2. Method of Analysis

Our method may be divided into two steps; first a filtration by a resonator having an assigned frequency f_0 is applied to ground vibrations recorded by three seismometers of the tripartite system; secondly, the correlation coefficient is computed between each pair of the filtered vibrations.

Suppose that two seismometers are placed as shown in Fig. 1 r meter apart from each other, and that a plane wave having velocity V and direction parallel to AB are passed through the place, the correlation coefficient corresponding to a particular frequency f_0 of the resonator will take the form,

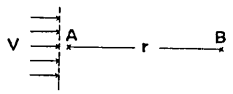

Fig. 1.

$$\rho(r, f_0)=\cos\left(2\pi\frac{rf_0}{V}\right). \qquad (1)$$

This equation shows that we can determine the value of velocity V by computing the correlation for various frequencies.

It was shown by Aki (1957) that Eq. 1 also holds for a dispersive wave only by the substitution of $V(f)$, velocity as a function of frequency, for the constant V.

Further, it was shown that if the wave is composed of partial waves having different velocities V_n's, the corresponding correlation coefficient will take the form

$$\rho(r, f_0)=\sum_n \frac{P_n(f_0)}{P(f_0)} \cos\left(2\pi\frac{rf_0}{V_n}\right) \qquad (2)$$

where $P(f_0)$ and $P_n(f_t)$ are the power of the composite wave and that

of the nth partial wave respectively.

If we do not know the direction of propagation of the wave in question, we need at least three seismometers in order to determine its direction and velocity. Supposing that a plane wave is propagated through the tripartite system as shown in Fig. 2, we shall have correlation coefficients for three pairs of seismometers as follows,

$$\left.\begin{aligned}\rho_{12}(r,f_0)&=\cos\left(2\pi\frac{r_{12}\cos(\theta_0-\theta_{12})}{V}f_0\right)\\ \rho_{23}(r,f_0)&=\cos\left(2\pi\frac{r_{23}\cos(\theta_0-\theta_{23})}{V}f_0\right)\\ \rho_{31}(r,f_0)&=\cos\left(2\pi\frac{r_{31}\cos(\theta_0-\theta_{31})}{V}f_0\right)\end{aligned}\right\}. \qquad (3)$$

Hereafter we shall call these correlation coefficients as functions of resonator frequency f_0 simply "correlation curves". Introducing a "characteristic frequency" f^*, which is defined by

$$\rho(r,f_0)=\cos\left(2\pi\frac{f_0}{f^*}\right) \qquad (4)$$

and which can be at once found by the inspection of correlation curve obtained, we can write the apparent velocities along the three lines as

$$\left.\begin{aligned}V_{12}&=\frac{V}{\cos(\theta_0-\theta_{12})}=r_{12}f_{12}^*\\ V_{23}&=\frac{V}{\cos(\theta_0-\theta_{23})}=r_{23}f_{23}^*\\ V_{31}&=\frac{V}{\cos(\theta_0-\theta_{31})}=r_{31}f_{31}^*\end{aligned}\right\}. \qquad (5)$$

If the values of f_{12}^*, f_{23}^* and f_{31}^* are found from the correlation curves, the velocity V and azimuthal angle θ_0 of wave propagation will be determined by the use of a graphical mothod as shown in Fig. 3 or that in Fig. 4. In both figures OP is the velocity vector giving the direction and velocity of wave.

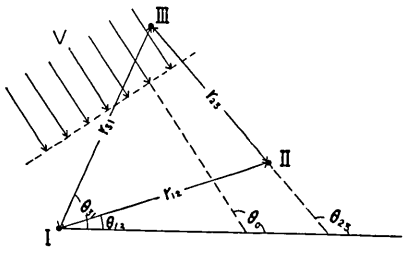

Fig. 2.

Here should be noted two essential differences between the direction determination by the present method and that by the ordinary "phase" method.

In the latter method, by observing the arrival times of a particular phase at three points, we get the apparent velocities

$$V_{12}=r_{12}/(t_1-t_2)$$
$$V_{23}=r_{23}/(t_2-t_3) \qquad (6)$$
$$V_{31}=r_{31}/(t_3-t_1)$$

From these equations and Eq. 5, it can be seen that the values of apparent velocities obtained by the spectral method cannot be negative,

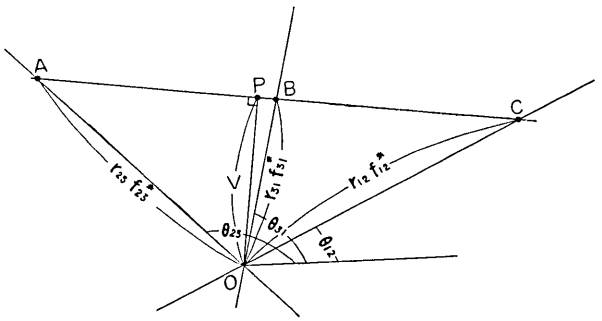

Fig. 3. Graphical determination of a velocity rector (OP).

while those determined by the phase method can be negative as well as positive. This means that the spectral method cannot give us the polarity of velocity vector, but the phase method can.

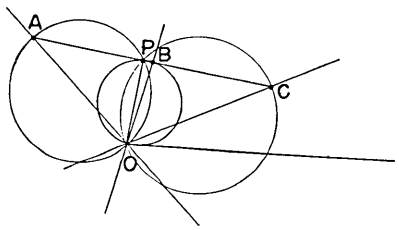

Fig. 4. Graphical determination of a velocity vector OP by the use of circles.

The other essential difference between the two methods is that the three apparent velocities are obtained independently of one another in the case of the spectral method, while those obtained by the phase method are dependent as seen from Eq. 6. In other words, by the use of the phase method we always get a definite velocity and direction even if the wave in question is not a plane wave. For instance, if the wave is a mixture of two waves having different velocities and directions of propagation, the application of the phase method, if possible at all, will yield a single direction and a single value of velocity which differ from those of the two component waves. On the other hand, in the spectral method, by examining the correlation curves and finding the two characteristic fre-

quencies corresponding to the two component waves from each of the curves, we can obtain velocity vectors for both waves, even though we cannot determine the polarity of vectors.

As we are using information involved in waves having a certain range of frequency, it is preferable that the frequency spectrum of the wave is flat over the range to be analysed. If the prevailing frequencies of wave have a narrow range, longer spans of tripartite should be taken. The choice of length of span also depends on the velocity value of wave to be studied and may be determined by the following relation

$$\frac{r\Delta f}{V}\approx 1 \qquad (7)$$

where Δf is the range of frequency over which the wave has enough power to be analysed.

3. Observation and Analyses

For the purpose stated in the preceding sections, we set up a tripartite system of seismometers in the grounds of Kamakura High School in August 1957 and made observations for about a month. Seismometers were placed in caves which were dug into a cliff of sandstone behind the school. A map of the tripartite site is shown in Fig. 5. The seismometers used are moving coil type transducers sensitive to vertical motion, and have free frequency of about 3cps.

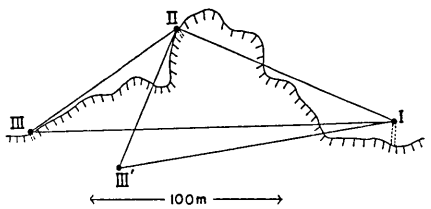

Fig. 5. Map of the tripartite site at the Kamakura High School.

Signals coming from the seismometers are sent to amplifiers through wires, and after appropriate amplification, are frequency modulated by carriers of audiofrequency.

The modulated signals are again frequency-modulated by carriers of about 400 Mc/s and sent from transmitters as radio waves to the receivers working at Aburatsubo which is located about 19 km apart from Kamakura. At the receiving station, after demodulation with respect to the carriers of 400 Mc/s seismometer signals are recorded on a magnetic tape having two tracks, in such a way that the signal modulated by the carrier of 2800 cps and that by one of two carriers having frequency 800 cps are recorded on

one of the tracks, and the signal modulated by the remaining carrier of 800 cps on the other.

In fact, for the present purpose we do not need the wireless part in the above arrangements. The use of this part in this study is merely due to the circumstance that the present observation is made as a part of a comprehensive study on seismicity of the Southern Kanto District conducted by Assoc. Prof. S. Miyamura of our Institute, and that the apparatus used is the UHF radio telerecording seismograph, RTS-II, made by S. Miyamura and M. Tsujiura[2] (1957).

The recording was made by using an endless reel having a very simple structure. The tape enclosed in the reel works as long as 7 minutes for a speed of 7.5 inches per second.

During the period of observation, the taperecorder is continuously in action waiting for an earthquake, and when one takes place, it is made to stop by means of a delayed trigger circuit after recording of waves.

The record of earthquake motions stored in the endless magnetic tape are brought to the laboratory, and analysed by the apparatus mentioned before. The filter used for this analysis is of phase shift type and its resonance frequency covers the range from 3.5 cps to 20 cps. Explanation of this filter and also of our correlation computer were given in the paper of K. Aki (1957) referred to before. Besides, in the analysis of an earthquake wave, we need an apparatus which can pick up a certain limited part of the seismogram, because as mentioned in the introduction, the analysis should be applied to the portion of the wave within which it can be assumed as stationary. For this purpose, we built an electromechanical gate which is opened and closed according to an assigned program thus controlling the operation of computer.

Practical procedures are as follows: at first we set the gate to open at the beginning of the portion of the seismogram to be studied and to close at its end; a pair of seismic signals, which are reproduced from the tape recorder and demodulated, are put into a pair of filters which are adjusted to have the same and assigned resonance frequency f_0 and Q value; after the filtration both signals are put into the correlation computer which works under the control of the gate; the result of computation is shown on the decatron indicators; and the same operation as above is applied to the other two pairs of signals.

2) S. MIYAMURA and M. TSUJIURA, *Bull. Earthq. Res. Inst.*, **35** (1957) 381–394.

Repeating the above procedures for various frequencies of the filter, we can obtain a set of three correlation curves, which indicate the characteristics of the wave portion in question in the way explained in the preceding section.

4. Interpretation of Actual Correlation Curves

As shown in Eq. 1, for the wave portion having a single definite velocity the correlation curve becomes a cosine function of the resonator frequency. The correlation curves obtained by actual earthquake wave parts, however, do not take such a simple form, but almost always indicate that they are composed of partial waves having different velocities in spite of the circumstance that the time intervals of the portion into which the waves are divided are taken as short as 1.5 to 3 seconds.

Typical examples of the curves are shown in Fig. 6a and Fig. 6b.

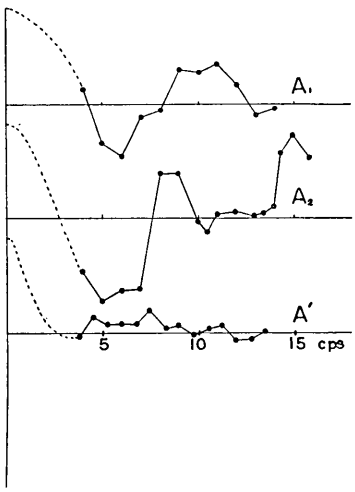

Fig. 6a. Typical correlation curves for wave portions having no component waves of high velocity.

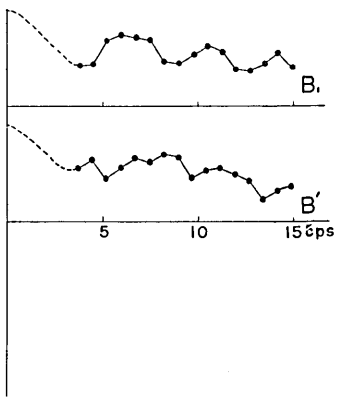

Fig. 6b. Typical correlation curves for wave portions involving high velocity waves.

There is a marked difference between the curves in Fig. 6a and those in Fig. 6b. Each of the latter curves are shifted upward from the zeroline, suggesting that the wave portion concerned has a partial wave of very high velocity. On the other hand the former curves do not indicate such a shift and run on the negative side as much as on the

positive.

Type A_1: Of the curves in Fig. 6a, the top one has a nearly sinusoidal form, even if the absolute values of the maximum and minimum are considerably lower than unity, and we can learn from them a single characteristic frequency f^*, referred to in Section 2. This type of curve is specified by A_1.

Type A_2: Sometimes, we can find two characteristic frequencies from a single curve. The second one in Fig. 6a is an example of this type. As can be seen from Eq. 2, the correlation curve for a wave consisting of two partial waves takes the form,

$$\rho(r, f_0)=\frac{P_1(f_0)}{P(f_0)}\cos\left(2\pi\frac{f_0}{f_1^*}\right)+\frac{P_2(f_0)}{P(f_0)}\cos\left(2\pi\frac{f_0}{f_2^*}\right) \qquad (8)$$

$$P(f_0)=P_1(f_0)+P_2(f_0)\ .$$

Therefore, if $P_1(f_0)$ and $P_2(f_0)$ vary with f_0 only slightly, we can obtain from the correlation curve the value of characteristic frequency and the fraction of power for each of the partial waves.

Type A': From such a curve as the bottom one in Fig. 6a, we can say nothing but that the wave portion is very complex, it is possibly composed of too many waves each having different velocity.

On the other hand, the curves in Fig. 6b may be classified as follows.

Type B_1: In a curve of this type, such as the top one in Fig. 6b, there are two characteristic frequencies; one is low and the other is very high. This type is frequently observed in the early parts of seismograms as will be shown in later sections. In most cases, the value of f^* for the high velocity wave cannot be determined because the spans of our tripartite are too short for such a wave, though appropriate for the low velocity waves.

Type B': From a curve such as the bottom one in Fig. 6b the characteristic frequencies can not be found for both low and high velocity waves, but the fraction of power for the high velocity wave can be estimated approximately by the inspection of the curve.

All of the correlation curves obtained can be classified into the above five types. The next step will be then to find velocity vectors by means of a graphical method such as shown in Fig. 3 or Fig. 4. If the wave portion investigated is an ideal plane wave, the points A, B and C in Fig. 3 should lie on a straight line which indicates the wave front, or the three circles in Fig. 4 should intersect at a point P. On the other

hand, if the wave is not unidirectional, the points in Fig. 3 will not lie on a straight line, nor will the circles in Fig. 4 intersect at a point.

In an actual earthquake wave, some of the wave portions are fairly well unidirectional, while others show departures from the ideal plane wave. The degree of departure from the ideal plane wave may be measured roughly by the area of hatched domain surrounded by three arcs such as shown in Fig. 7. If the wave portion is perfectly unidirectional this domain is reduced to a point.

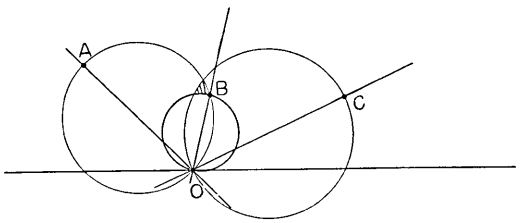

Fig. 7. The degree of departure from the ideal plane wave may be measured roughly by the area of hatched domain.

It happens, though not often, that for a particular wave portion the three correlation curves corresponding to three seismometer pairs can not be classified as the same type; for instance, one of them is of type A', while the other two are both of type A_1. As can be seen in Fig. 8, if we know only two of three characteristic frequencies, we can not determine whether the line AB or AB' is the actual wave front, and we have two possible vectors, OP and OP'.

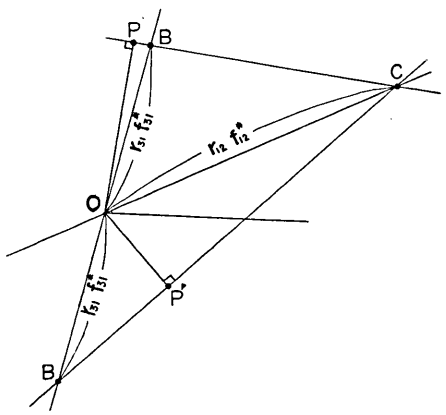

Fig. 8. Possible two velocity vectors OP and OP'.

In the following sections, the correlation curves for individual earthquake will be interpreted, and the following points will be investigated.

1. *General features* The general features of correlation curves are described with reference to the original seismograms from which the curves are reduced.

2. *High velocity waves* The value of velocity and the fraction of power for the high velocity waves are investigated.

3. *Velocity vectors of low velocity waves.* Velocity vectors are derived for low velocity waves whenever possible. If a wave portion is not unidirectional, the degree of departure from the ideal plane wave will be measured roughly by the area of domain surrounded by arcs

such as shown in Fig. 7. When we can get only two of three characteristic frequencies for a particular wave portion, two possible vectors are shown with question marks as in Figs. 12, 16, and 20.

It should be noted here again that we can not determine the polarity of velocity vectors in any case only by the spectral method. Our velocity vectors will be plotted on a half plane instead of a full plane.

5. Earthquake of Aug. 11, 1957.

General feature. Original seismograms, obtained from the seismometers placed at the points I, II, and III in Fig. 5, are shown in

Tabl. 1. The characteristic frequency f^*, apparent velocity V along each line, and ratio of power borne by component waves.

	I—III			II—III			I—II		
Wave portion	f^* (cps)	V (mps)	Power ratio	f^* (cps)	V (mps)	Power ratio	f^* (cps)	V (mps)	Power ratio
1	70 10	13,600 1,950	0.7 0.2	high		~1.0	high		0.8
2	5.4 high	1,050	0.4 0.2	high 6.2	590	0.4 0.4	high 3.0	375	0.6 0.2
3	high 13	2,530	0.4 0.1	high 6.0	570	0.5 0.1	high 11	1380	0.6 0.2
4	39 2~3	7,600 400~600	0.8 0.1	high 5.4	520	0.3 0.2	high 5~6	630~750	0.7 0.1
5	3	590	0.2	5.2	500	0.2	6.5	820	0.2
6	3.7	720	0.3	?		?	high 5.2	650	0.4 0.2
7	3	590	0.2	6	570	0.2	5 high	630	0.3 0.3
8	?		?	4	380	0.1	?		?
9	?		?	3	290	0.1	6.7	840	0.3
10	7	1380	0.2	5	480	0.1	2~4 12	250~500 1,500	0.3 0.2

Fig. 9. The analysis is made of ten portions into which the seismograms are divided as shown in Fig. 9; each portion covers 3 seconds. Correlation curves from them are shown in Fig. 10. At first sight, it can be seen that none of their forms is simply sinusoidal as is expected for an unidirectional wave having a single definite velocity. The curves for the earlier portions of the seismogram are of the types B_1 and B', while for the later portions the types A_1, A_2 and A' are predominant.

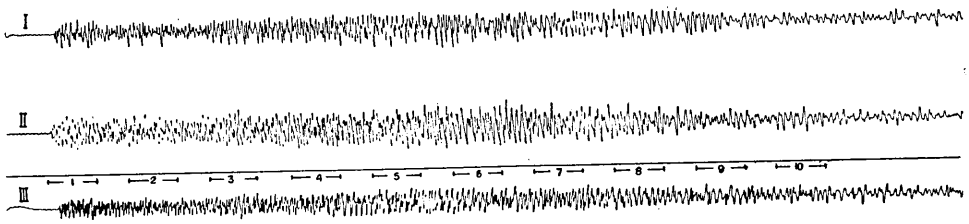

Fig. 9. Seismograms of the earthquake of Aug. 11, 1957.

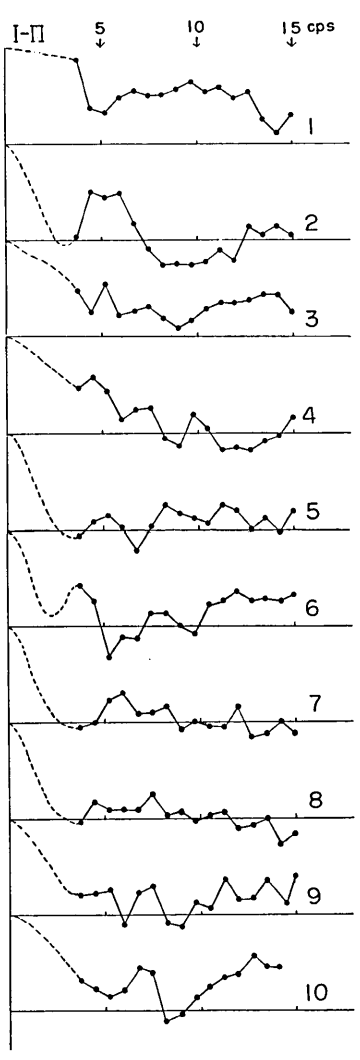

Fig. 10a.

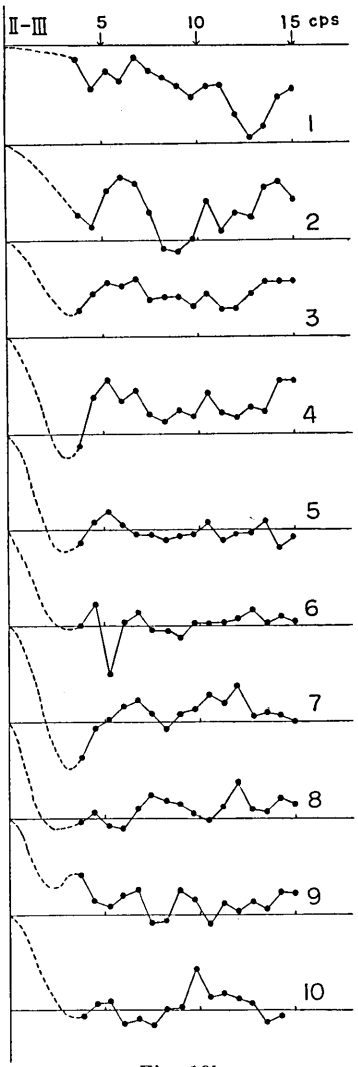

Fig. 10b.

By the inspection of these curves, the characteristic frequency and the fraction of power are found for each partial wave discernible in the respective curve and are listed in Table I. In the table are also shown the apparent velocities of waves along the three lines, which are obtained by the use of Eq. 5.

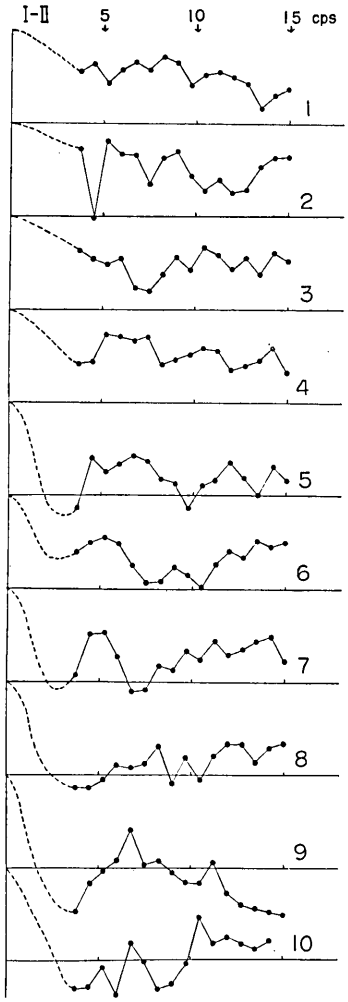

Fig. 10c.

High velocity waves. It can be seen from Table I that the high velocity wave is predominant in the earlier portions of the seismogram and disappear in its coda portions. In Fig. 11 the fraction of power borne by the high velocity wave is plotted against the time from the initial motion. As clearly shown in this figure, the high velocity wave is most predominant in the first portion, and decreases in power with time, and again begins to predominate in the fourth portion, possibly indicating the arrival of the S wave within this portion. This identification is justified from the epicentral distance reported by the meteorological observatory,

On the other hand, in the portions following the fifth portion the high velocity wave almost disappears. It is interesting to observe that these portions are relatively larger in amplitude than the preceding portions as shown in the seismograms.

The velocity of high velocity wave is often too high to be determined from the present analysis; this is partly owing to the lack of power in the waves in their range of frequency high than 15 cps and partly due to too short a length of span being taken for such waves.

This velocity, as well as direction of propagation, may be deduced from the arrival times of initial motion. Although this attempt also failed, because the arrival times for three seismometers coincide with each other within the range of error caused by the vagueness of the initial motion itself,

it was found the velocity can not be lower than 5 kmps.

The ratio V_p/V_s, however, can be learned from the obtained apparent velocities of the first and fourth parts along the line I–III; they are 13.6 and 7.6 kmps respectively. The ratio is 1.79, which is very close to the values obtained by the use of travel time curves of P and S waves of near earthquakes, by Sagisaka (1931), Honda (1931) and Sagisaka and Takehama (1935).

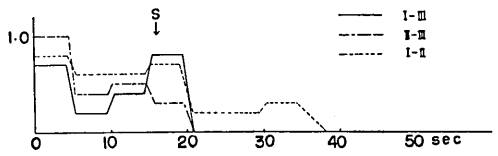

Fig. 11. The fraction of power borne by high velocity waves plotted against the time from the initial motion.

This earthquake was observed by the seismometer network of local meteorological observatories, and its epicenter is reported to be located in the sea off Boso Peninsla at latitude 34.2°N and longitude 140.3°E. This epicenter is in the direction S 35°E and about 150 km apart from our tripartite station.

If the high velocity wave is coming from the epicenter as a plane wave, using the above direction we can obtain the velocity values for the first and fourth portions, of which the apparent velocities along the line I–III are known. It was found that the velocity of the first portion is 7.4 kmps and that of the fourth 4.1 kmps, reasonable ones for P and S wave refracted critically at the Mohorovicic discontinuity.

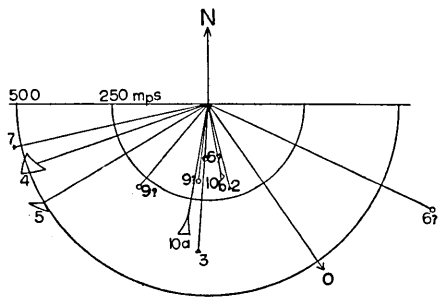

Fig. 12. Velocity vectors for low velocity waves.

Velocity vectors of low velocity waves. The velocity vectors of low velocity waves are obtained by the graphical method as illustrated in Fig. 4 and Fig. 7, and shown in Fig. 12. The area of domain surrounded by three arcs roughly measures the degree of departure from the ideal plane wave as referred to in the preceding section. The number attached to each vector indicates the number of the wave portion. For the sixth and nineth portions, only two of three characteristic frequencies are found, and two possible vectors with question marks are shown for each of them in Fig. 12. We could not find the vector for the first portion and for the eighth which are of the type B' and A' respectively.

Fig. 12 shows that the directions of low velocity waves can be grouped into two; one is nearly N–S direction, and the other is nearly N 70°E–S 70°W. The portions 4, 5 and 7 belong to the latter, and their velocities are around 500 mps. On the other hand, the portions 2, 3, 10a, 10b and possibly 6 and 9 point to the N–S direction, and the velocity value ranges from 150 mps to 400 mps.

It can be seen that none of the vectors point to the epicenter reported by the meteorological observatory; the direction of the epicenter is shown in the figure with the symbol *O*. The departure of their directions from the epicenter direction is very notable, but is not impossible to explain. Their velocities are around or lower than 500 mps, and the ranges of frequency is from 3 cps to 15 cps, so that their wave lengths are less than two hundred meters. Those waves must be generated at a very shallow part of the crust by the incidence of primary waves coming from the origin of earthquake, and have travelled through the shallow part to the observation point. Thus the topographical and geological heterogeneities over the very shallow part of earth's crust may cause notable refraction and scattering of the waves in the horizontal plane.

As will be seen in the following sections, the low velocity wave having direction of propagation nearly N–S and velocity value around 350 mps exists also in other earthquakes, therefore it is possible that there is a certain place at which secondary waves having a definite character are always generated after the incidence of primary waves.

6. Earthquake of Aug. 23, 1957

General features. Original seismograms obtained by the same tripartite station as the preceding one are shown in Fig. 13. The analysis

Table 2. The characteristic frequency f^*, apparent velocity V along each line, and ratio of power borne by component waves.

	I—III			II—III			I—II		
Wave portion	f^* (cps)	V (mps)	Power ratio	f^* (cps)	V (mps)	Power ratio	f^* (cps)	V (mps)	Power ratio
1.	high		~1.0	high 5.5	530	0.8 0.2	high 6	750	0.6 0.3
2.	60 6.5	11,700 1,270	0.8 0.2	high		~1.0	66	8,300	0.8
3.	high		0.4	high		0.5	high		0.6
4.	60 5	11,700 980	0.4 0.3	high 5.5	530	0.7 0.2	high		0.4
5.	9.5	1,850	0.4	5.5	530	0.4	9.0	1,130	0.4

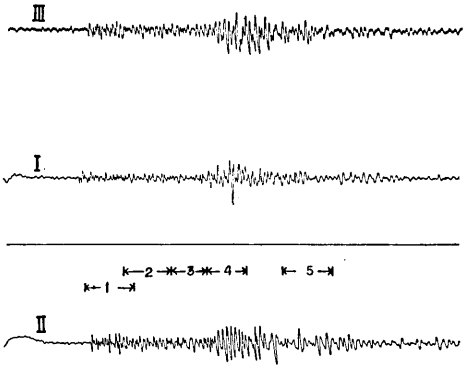

Fig. 13. Seismograms of the earthquake of Aug. 23, 1957.

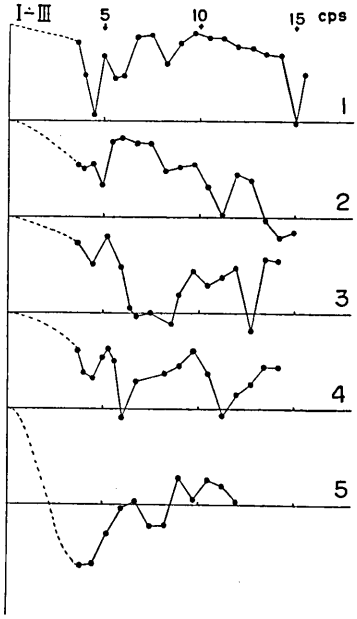

Fig. 14a.

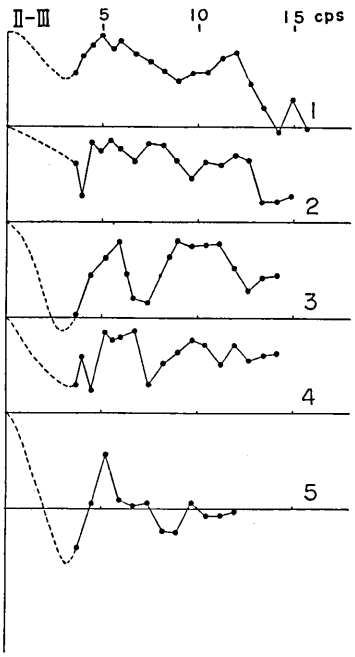

Fig. 14b.

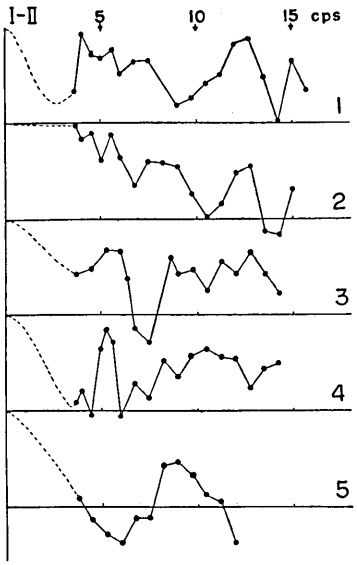

Fig. 14c.

is made of five portions into which the seismograms are divided as shown in Fig. 13. Correlation curves for them ares hown in Fig. 14. In a similar way to that of the preceding example, the characteristic frequency and fraction of power are deduced for each partial wave discernible in every curve, and listed in Table 2 with the corresponding apparent velocity.

High velocity waves. The fraction of power borne by the high velocity wave is plotted against the time from the initial motion in Fig. 15. It is clear that the high velocity wave is predominant in the ealier portion of seismogram and later disappears. In this case such an increase of power at the arrival of the S wave as observed in the preceding example can not be seen; the arrival of the S wave is found in the third part by the inspection of the original seismograms. This fact may be explained by supposing that the duration of event at the origin of earthquake is considerably long, may be three to five seconds, and therefore in the case of short P–S duration the power of high velocity wave can not decrease in the portion preceding the arrival of the S wave.

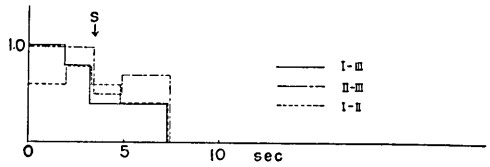

Fig. 15. The fraction of power borne by high velocity waves plotted against the time from the initial motion.

In this example, the velocity of high velocity wave is found for the second portion of seismogram. As shown in Table 2, two of the three characteristic frequencies are estimated from the curves, and though the remaining one can not be determined exactly, it is found to be at least larger than 60 cps. The two known characteristic frequencies can give us two possible vectors. If the wave is unidirectional, from these two possible vectors two values of the remaining characteristic frequency can be derived; they are found to be 29 cps from one of the vectors, and 123 cps from the other. The former can not be allowed, because this characteristic frequency con not be lower than 60 cps. Thus the latter gives the actual velocity vector for this high velocity wave; the value of velocity is determined as 7.6 kmps, a reasonable one for P wave, and the direction N 43°W–S 43°E.

For the rest of the above portion, we could not find the velocity of the high velocity wave. Also the arrival times of initial motion tell us nothing but that the velocity can not be lower than 5 kmps.

This earthquake was not registered by the network of local meteorological observatories. The observed *P–S* duration of this earthquake is 4 seconds, and its epicenter is very near our tripartite station.

Velocity vectors of low velocity waves. As shown in Fig. 15, the high velocity wave is so predominant over the whole duration of seismogram expect for the coda part, that the low velocity wave often does not have enough power to indicate clearly its characteristic frequency in the correlation curves. Therefore, a complete set of characteristic frequencies can be found only for the fifth portion, and for the first and fourth portion only two of three characteristic frequencies are found from each set of correlation curves. Fig. 16 shows the velocity vectors for the above three portions ; one vector for the fifth portion and two possible vectors for each of the first and fourth portions.

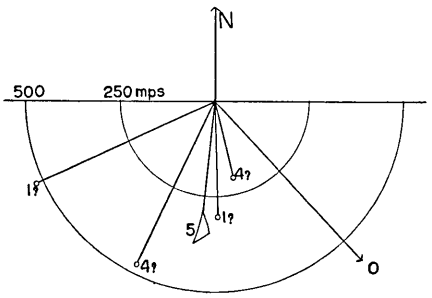

Fig. 16. Velocity vectors for low velocity waves.

It is remarkable that the direction of propagation of the fifth wave portion is nearly N–S, which was also the direction of a group of wave portions found in the preceding example. Besides, the velocity value of this portion coincides well with those of the third and tenth parts of the seismogram investigated in the preceding example.

In previous paragraphs, the velocity of the high velocity wave was found as 7.6 kmps. At the same time its direction of propagation was also determined. This direction is shown in Fig. 16 with the mark *O*. Since this direction can reasonably be assumed as pointing to the epicenter of this earthquake, it can be said that none of the directions of low velocity waves coincides with the direction pointing to the epicenter of the earthquake.

7. Earthquake of Aug. 25, 1957.

This earthquake was observed by the tripartite system (I, II, III′) in Fig. 5, instead of the system (I, II, III) used in the above two cases. The point III′ is not situated on hard sandstone bed, but is on rather soft ground. As will be shown later, this alteration of site caused a remarkable decrease in fraction of power of the high velocity wave for

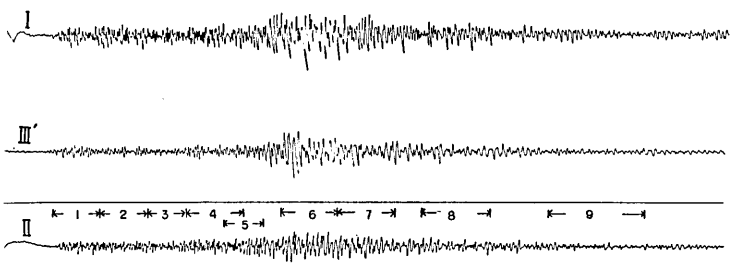

Fig. 17. Seismograms of the earthquake of Aug. 25, 1957.

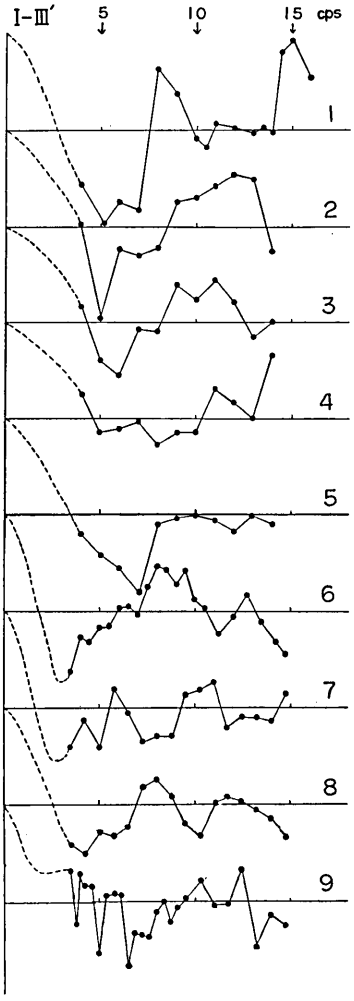

Fig. 18a.

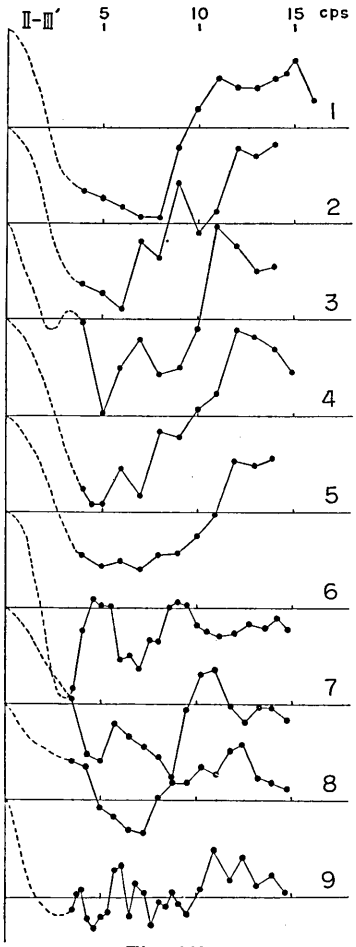

Fig. 18b.

the seismometer pairs (I III′) and (II III′).

General features. Original seismograms are shown in Fig. 17. Each of them are divided into nine portions, as shown in the figure. Correlation curves are obtained for these portions and shown in Fig. 18. It can be seen that the forms of curves for the seismometer pair (I, II) resemble those found in the preceding examples, except that near 10 cps an abnormal negative value of correlation coefficient is observed, which may be due to a local abnormal vibration at the place. While, in all of the curves for the seismometer pairs (I, III′) and (II, III′) the high velocity wave is not discernible. This fact shows that low velocity waves are exceedingly predominant at the surface of a soft layer even in the earlier parts of seismogram. It is interesting to observe on the seismograms shown in Fig. 18 that the intial motions recorded at the points, I and II begin suddenly, while at the point III′ (soft ground) the commencement is slow and vague.

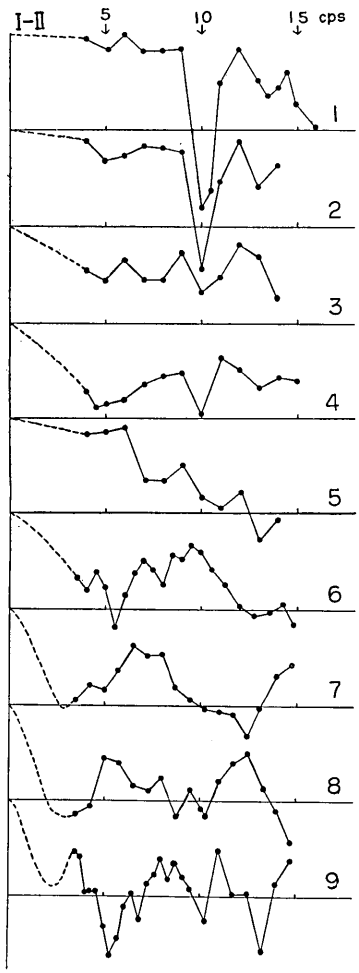

Fig. 18c.

In a similar way as in the preceding examples, the characteristic frequency and fraction of power are found for each partial wave discernible in every curves and listed in Table 3 with the corresponding apparent velecity.

High velocity waves. The fraction of power borne by the high velocity wave found in the curves for the seismometer pair (I, II) is plotted against the time from the initial motion in Fig. 19. It can be seen that the high velocity wave is most predominant in the first portion after which it gradually decrease in power and again predominates in the fifth portion which is identified as the *S* wave on the original seismograms. In the portions following the fifth, the high velocity wave is, if not absent, feeble.

In this case, the velocity of the high velocity wave could not be determined except that the apparent velocity of the wave portion identified as the S wave along the line (I II) is estimated as 6.0 kmps.

Table 3. The characteristic frequency f^*, apparent velocity V along each line, and ratio power borne by component waves.

	I—III			II—III			I—II		
wave portion	f^* (cps)	V (mps)	Power ratio	f^* (cps)	V (mps)	Power ratio	f^* (cps)	V (mps)	Power ratio
1.	8.0 12.0	1,170 1,760	0.4 0.4	13.0	1,020	0.6	high		~1.0
2.	11.5	1,690	0.6	12.0	940	0.8	high		~1.0
3.	10.0	1,470	0.5	12.0 3.5	940 280	0.6 0.3	high 3.0	 380	~0.6 0.2
4.	16.0	2,350	0.2	12.0	940	0.9	high 10.0	 1,250	0.4 0.2
5.	10.0	1,470	0.4	13.0	1,020	0.5	48. 3.0	6,010 380	0.9 0.1
6.	8.0	1,170	0.6	4.5	350	0.5	high 9.5	 1,190	0.4 0.3
7.	5.5	810	0.2	11.0 6.0	870 470	0.2 0.2	high 7.0	 880	0.4 0.4
8.	8.0	1,170	0.5	12.0	940	0.4	5.5 high	690 	0.3 0.2
9.	low 11	2,600	0.3 0.1	low		0.2	3.5	440	0.5

Velocity vectors of low velocity waves. Since one of the seismometers is placed on a soft ground, the type of correlation curves obtained are so different according to seismometer pairs, that the reduction of velocity vectors is rendered considerably difficult. Although complete sets of characteristic frequencies are found for portions, 3, 4, 5, 6, and 8, only the sixth portion, and possibly also the eigth portion, is an unidirectional wave. The rest of them show considerable departure from the ideal plane wave as indicated in Fig. 20. On the other hand, for the portions, 1, 2, and 7, only two of three characteristic

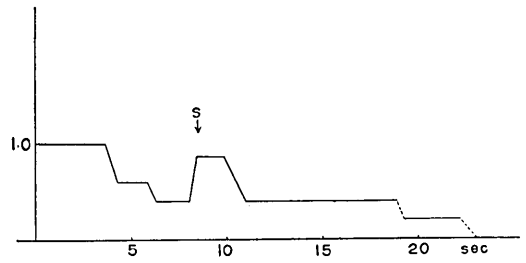

Fig. 19. The fraction of power borne by high velocity waves plotted against the time from the initial motion.

frequencies are obtained and two possible vectors are shown for each of them.

The velocity vector of the sixth portion, found as unidirectional, has nearly the same direction and velocity value as those for the fifth wave portion of Earthq. of Aug. 23, the third and tenth portion of Earthq. of Aug. 11.

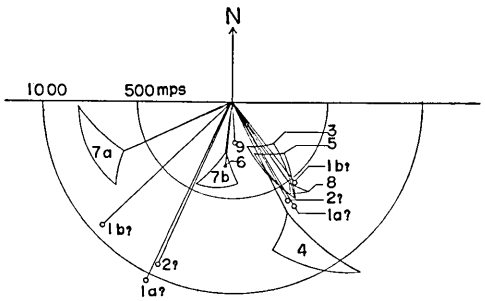

Fig. 20. Velocity vectors for low velocity waves.

On the other hand, many of the velocity vectors in Fig. 20 come together around the direction N 34°W–S 34°E, and their velocity value are about 500 mps, which is also observed in one of the two groups of low velocity waves found in our first example.

This earthquake wave was recorded at five stations; three local meteorological observatories and two stations of the Earthquake Research Institute located in and near Kanto district. Of the five stations, *P–S* times are available only at two; Tsukuba and Matsushiro stations. The *P–S* time is 13.4 sec at Tsukuba and 20.9 at Matsushiro; it is 9 sec at our station. In order to find the epicenter, we used Sagisaka-Takehana's table in which *P–S* times are given for various focal depths and epicentral distances, but we could not determine a well defined epicenter for any choice of focal depth. What we can say about the epicenter of this earthquake is only that it lies in the land area, possibly in a direction N slightly W from our tripartite station.

It is not impossible that the direction N 34 W–S 34 E, around which many of the velocity vectors come together, is pointing to the epicenter of this earthquake. But this seems unlikely, because if the high velocity wave identified as the *S* wave, of which an apparent velocity is known, is propagated in this direction, its velocity should exceed 5 kmps, perhaps too high for the *S* wave.

8. Earthquake of Aug. 29, 1957.

This earthquake wave was recorded by the tripartite system (I II III) in Fig. 5, but in this case the vibration of seismometer at the point I was not recorded well on the magnetic tape. Therefore, the velocity

vectors could not be obtained for this earthquake.

General features. In Fig. 21 are shown original seismograms, which seem, at first sight, to suggest that there was two earthquakes in succession. These seismograms are divided into twenty six portions; each covers 5 seconds. Correlation curves for these portions are obtained for the seismometer pair (II III), and shown in Fig. 22. From the comparison of these curves with the original seismograms in Fig. 21, it is found that the wave portions following the initial motion are remarkably different in form of correlation curve from those following the fifteenth part, in spite of the similarity found between them in general appearance on the seismogram. This fact is clearly indicated in Fig. 23, which shows the fraction of power borne by high velocity wave. The high velocity wave is predominant over the portions from the first to the sixth, while hardly discernible in the portions after the fifteenth portion. The former wave portions may be bodily waves coming from underneath the crust, while the latter may be surface waves. Between these two main wave groups, we can find wave portions having a single low velocity such as the seventh and eighth portions, as well as those being comparatively rich in power of high velocity wave such as the nineth, eleventh, and thirteenth portions, each followed by wave portions being not so rich in it.

Taking into account the results obtained in the preceding example, let us examine whether the whole seismogram is due to two earthquakes which occurred in succession or due to one single earthquake. If the former is the case, the portions from the first to the nineth must be considered as caused by the earlier earthquake, aud the remaining portions as caused by the later one, because in the tenth portion contains a considerable amount of high velocity wave, which is not prevailing in the coda portions of earthquakes hitherto analysed. Then, the general appearances of the original seismogram suggests that the S wave of this earlier earthquake may be found in the first portion or the second. Thus we must have for this earthquake an unusual seismogram, in which the duration of high velocity wave is too long for the short P–S duration.

It seems more natural to suppose that the seismogram is due to a single earthquake; the portions from the first to the sixth are the P wave, the one or all of the nineth, eleventh and thirteenth is the S wave, and the portions following the fifteenth are surface waves. Then this earthquake must be considered as a rather distant and comparatively

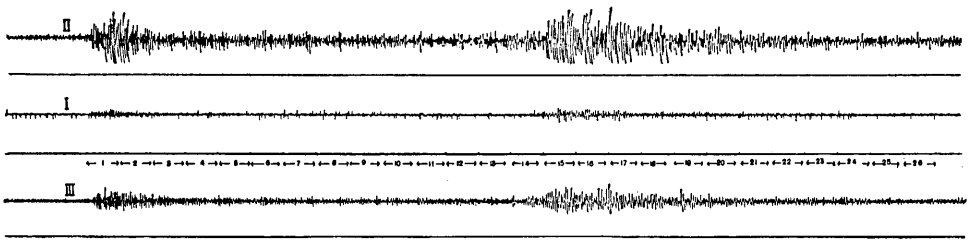

Fig. 21. Seismograms of the earthquake of Aug. 29, 1957.

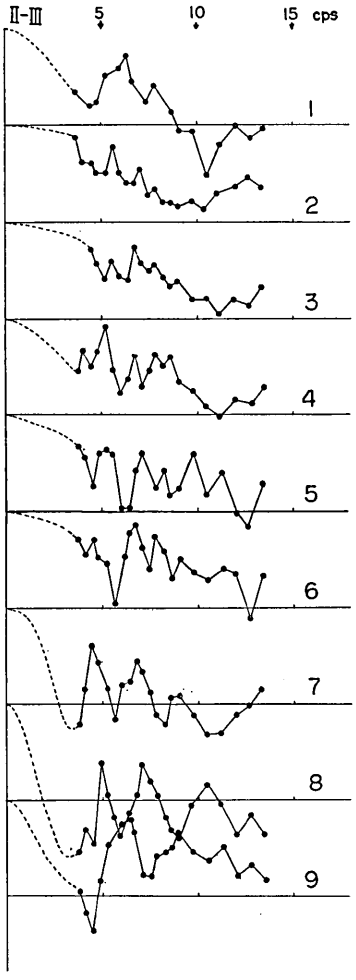

Fig. 22a.

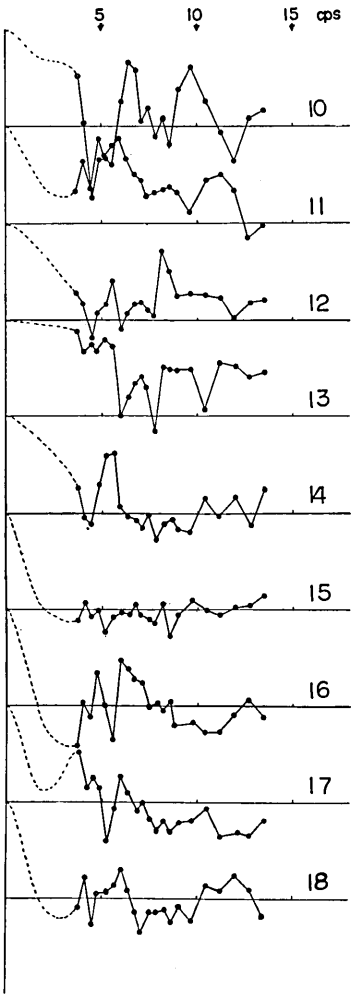

Fig. 22b.

large one. The long duration of the high velocity wave at the earlier portions of seismogram may be explained partly by the long duration of event at the origin owing to the largeness of the earthquake, and partly by the variety of wave paths associated with the long epicentral distance.

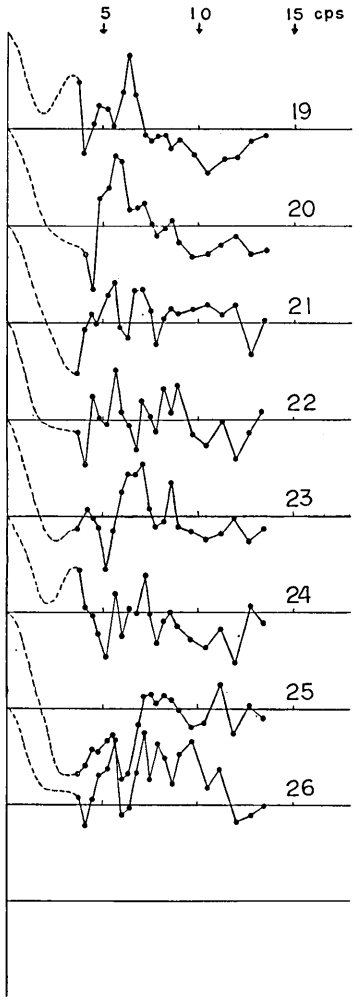

Fig. 22c.

In fact, this was due to a single earthquake, which according to the observation network of local meteorological observatories, is reported to be a deep focus earthquake occurring at latitude 29°3/4 N, longitude 139°1/4 E, and at a depth about 450 km.

In the determination of focus by the meteorological observatories, however, the *S* wave seems to be found in the fifteenth part, which we considered as a surface wave because there is no high velocity wave in it. Although it is widely believed that earthquake waves of deep focus are not accompanied by surface waves, it will be important to make more detailed investigations of this matter especially in the higher range of frequency.

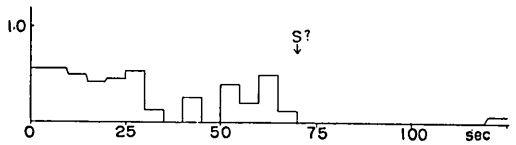

Fig. 23. The fraction of power borne by high velocity waves plotted against the time from the initial motion.

9. Microtremors

Microtremors which exist steadily as a background noise are recorded by the tripartite (I II III) in Fig. 5, and analysed in the same way as in the preceding examples. Fig. 24 shows correlation curves for the three seismometer pairs. We can see that the high velocity wave

is discernible in the curve for the pair (I II), though hardly in those for the remaining pairs. This high velocity may be an apparent one due to a part of microtremors being propagated in the direction nearly perpendicular to the line (I II).

This fact is interesting as compared with the nature of microtremors in the city area. Microtremors observed at Hongo, in Tokyo, by Aki (1957) have almost uniform power in every direction of propagation.

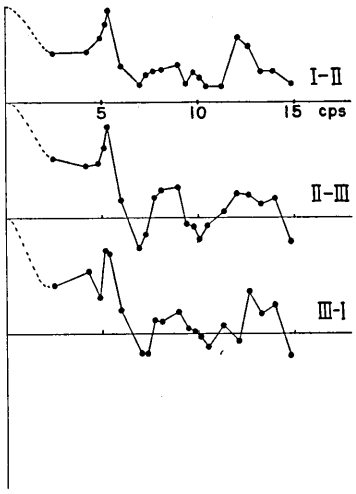

Fig. 24. Correlation curves for microtremors.

10. Summary and discussion

From the investigation of individual earthquake waves by the spectral method, we have found several interesting facts about their chaotic parts. It should be noted here that those facts revealed are all concerned only with wave having frequencies higher than 3 cps, and any conclusion from them can not be applied at once to those having lower frequencies. The first fact is that in a seismometer placed on a relatively hard surface such as sandstone, two kinds of waves are predominant; of which one has a high velocity of several kilometers per second, and the other has a low velocity of several hundred meters per second. The high velocity wave is most predominant in the initial portion of seismogram, and decreases in power gradually until the beginning of the S wave, where it again become predominant. In the portions, after the S wave the high velocity wave almost disappears.

The velocity of this high velocity wave appearing in the P–S interval was found in one case as 7.6 kmps, and in another case as 7.4 kmps. The velocity of the high velocity wave identified as S wave was found as 4.1 kmps. Those high velocity waves possibly have their origins at a deeper part of the earth's crust, whether the origins may be primary ones which is actual origins of earthquakes, or secondary ones such as the Mohorovičič discontinuity which generates refracted or reflected waves.

On the other hand, the low velocity waves must be considered as originating at the shallow part of crust. They may be classified into

two groups according to whether the origins are near the epicenters or near the observation station. A surface wave that is generated around the epicenter and propagated from there to the station belongs to the former, while the local vibration of surface layer generated by the incidence of primary wave coming from the origin of earthquake belongs to the latter. The existence of a low velocity wave of the latter type is most strongly confirmed in the record of a seismometer placed on a surface of soft soil (Earthq. of Aug. 25.). In this case, the high velocity wave is not discernible even in the initial portion, and the low velocity wave is predominant all over the seismograms.

It was found that the directions along which the low velocity waves are propagated are different among wave portions of a seismogram, and none of them point to the origin of earthquake. Further, wave portions having a common direction and a common value of velocity are found in every earthquake wave investigated. It is interesting that this common direction is perpendicular to the coast line near the observation station.

It is expected that the duration of the high velocity wave has some bearing upon the duration of event at the earthquake origin. No conclusion, however, can be drawn here because the number of records obtained is insufficient. It is also expected that the study along this line will make possible a sound estimation of energy of chaotic earthquake waves based on the investigation of separate powers carried by waves of different types. We hope that these important problems will be solved by applying the present method to a tripartite system having longer spans and determining the exact values of velocity and fraction of power for high velocity waves which are discernible in every portion of seismogram.

The present study is essentially a preliminary one in which are presented suggestions of several interesting problems solvable by the spectral method rather than conclusions to those problems.

The lengths of spans of the tripartite system should be chosen as appropriate to the waves to be studied. Those chosen in the present investigation are too small for the high velocity waves but appropriate for the low velocity waves in the range of frequencies as investigated in the present study.

Though it is not so easy to expand the range of frequency to the lower side, this expansion is necessary for the fuller understanding of earthquake waves, especially of the surface waves.

In order to draw conclusions about the nature of chaotic parts of

earthquake waves, we are preparing for a further study of near earthquake waves, with improvements in equipment and an appropriate choice of both the place and the length of span of tripartite system. In the next attempt, we are going to use a double tripartite system of seismometers, in which one tripartite having longer spans is for the high velocity waves and the other for the low velocity waves.

11. Acknowledgement.

The writers express their thanks to Prof. Chuji Tsuboi of the Geophysical Institute, Tokoy University for his constant guidance and encouragement as well as his valuable suggestions made in preparing the manuscript.

The writers' thanks are also due to Assoc. Prof. Setumi Miyamura of our Institute for his kind help and valuable advices made in the course of investigation, especially in the operation of seismograph systems developed by him without which the present work could not be carried out.

---

5. 近地地震波動のスペクトル的研究 (1)

地震研究所 安芸敬一 辻浦賢 堀実 後藤健一

近地地震波動は一般に極めて複雑であつて，その任意の部分の波としての性質を明らかにするには，これまでの走時解析を用いる位相的な立場からの研究だけでは不充分だと思われる．この論文では，前に著者の一人が微動の解析に用いた方法，即わち波動を時間的にフーリエ分解し，分解された成分波について空間相関をしらべるという方法を，近地地震波に応用した．

地震波の記録には，宮村・辻浦の極超短波無線地震計RTS IIを用い，3 cps の上下動地震計3台を鎌倉高校の裏庭に設置した．地震波形は無線によつて油壺に送られ，そこで 2-track のテープレコーダーに記録された．解析は研究室においてデカトロン相関器と位相ロ波器を用いて行われた．

8月一杯の観測で解析されうる地震記録が 4 組得られた．数は少ないが次のような興味深い事実が明らかにされた．但し次の事実は周波数範囲 3cps から 15cps の間の地震波動について得られたものである．

1. Sandstone のような比較的固い地表上に地震計をおいて記録した波動には 2種類の波，1つは数粁毎秒の伝播速度をもつ速い波，1つは数百米毎秒の伝播速度をもつ遅い波が現われる，速い波は記象の最初の部分に最も卓越し，その後次第に減少して，S波の到来する時間にまた著しくなる．S波のあとは速い波の含まれる割合は殆んど零になる．

2. p～s 間に表われる速い波の伝播速度は，ある地震の場合に 7.6 kmps, 他の地震で 7.4 kmps

であつた．S 波のところに表われる速い波の伝播速度は 4.1 kmps であつた．

3. 遅い波は，震央付近で発生し観測点まで伝播して来た表面波か，あるいは震源から直接くる波によつて観測点近くの地表に 2 次的に生じた局地的振動の一種であろう．この後者の型の波の存在は，比較的やわらかい表土上に地震計をおいたとき (8月25日の地震)，もつとも著しく認められた．こういう表土の上におかれた地震計の記録には速い波の占める割合が P波の初めから，尾部に到るまで殆んど零であつた．

4. 遅い波の伝播方向は一般に真の震源の方向からはずれており，そのなかにはどの地震にも共通に，同じ伝播速度と方向をもつ波が見出された．速度の大きさは，350 mps, 方向は南北に近く，その方向が観測点近傍の海岸線と直角になつていることは興味深い．

5. この研究では三点観測の span が，速い波の速度をもれなく決めるのに充分な程長くなかつたので，その性質をくわしく調べられなかつた．近い将来，大きい三角点と小さい三角点とを併用して，速い波と遅い波について一層くわしい研究をする予定である．